Figure S1

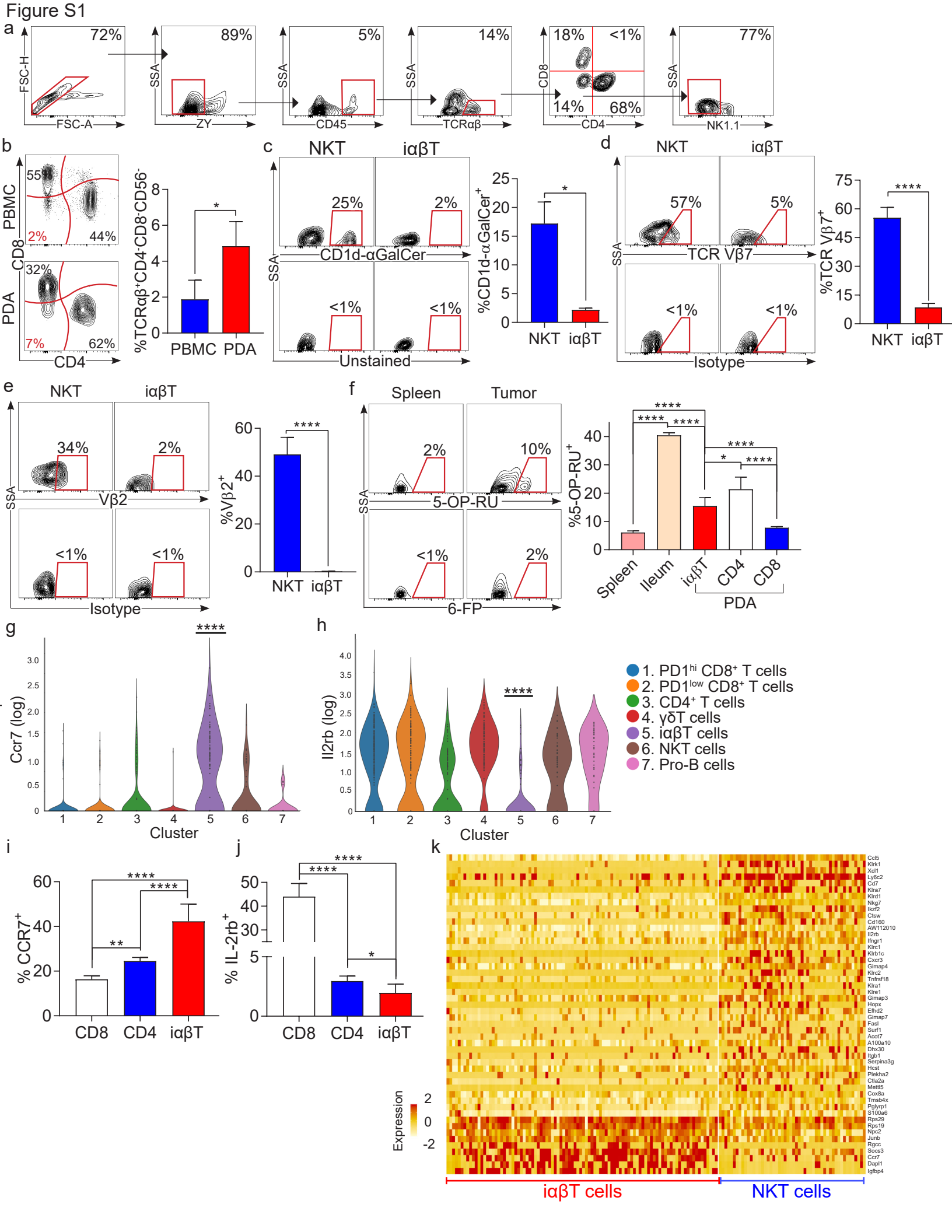
a
72%
89%
5%
14%
18%
<1%
14%
68%
77%
FSC-H
FSC-A
SSA
ZY
CD45
TCRαβ
CD8
CD4
NK1.1
b
PBMC
PDA
CD8
CD4
55%
2%
44%
32%
7%
62%
%TCRαβ+CD4-CD8-CD56-
PBMC
PDA
c
NKT
iαβT
25%
2%
<1%
<1%
CD1d-αGalCer
Unstained
%CD1d-αGalCer+
d
NKT
iαβT
57%
5%
<1%
<1%
TCR Vβ7
Isotype
%TCR Vβ7+
e
NKT
iαβT
34%
2%
<1%
<1%
Vβ2
Isotype
%Vβ2+
f
Spleen
Tumor
2%
10%
<1%
2%
5-OP-RU
6-FP
%5-OP-RU+
Spleen
Ileum
iαβT
CD4
CD8
PDA
g
Ccr7 (log)
Cluster
h
Il2rb (log)
Cluster
1. PD1hi CD8+ T cells
2. PD1low CD8+ T cells
3. CD4+ T cells
4. γδT cells
5. iαβT cells
6. NKT cells
7. Pro-B cells
i
% CCR7+
CD8
CD4
iαβT
j
% IL-2rb+
CD8
CD4
iαβT
k
Expression
iαβT cells
NKT cells

Figure S1. iαβTs do not express NKT-specific TCR chains or associated surface markers. (a) Live singlet $CD45^+$ leukocytes from day 21 orthotopic KPC tumors and spleens in WT mice were gated for further analysis as shown in Figure 1a. **(b)** $CD45^+TCR\alpha\beta^+CD56^-$ leukocytes from pancreatic tumors and PBMC of PDA patients were gated and tested for expression of CD4 and CD8. Representative contour plots and quantitative data are shown (n=5 patients). **(c)** Murine $CD45^+TCR\beta^+CD4^-CD8^-NK1.1^-$and $CD45^+TCR\beta^+CD4^-CD8^-NK1.1^+$ cells were stimulated with α-GalCer and tested for expression of the α-GalCer:CD1d complex. **(d, e)** PDA-infiltrating murine $CD45^+TCR\beta^+CD4^-CD8^-NK1.1^-$ and $CD45^+TCR\beta^+CD4^-CD8^-NK1.1^+$ cells were each gated and tested for expression of (d) TCR Vβ7 and (e) TCR Vβ2 compared to isotype control. Representative contour plots and quantitative data are shown. **(f)** Murine $CD45^+CD3^+CD4^-CD8^-NK1.1^-$ cells were isolated from spleen, ileum, and PDA and $CD4^+$ and $CD8^+$ T cells were isolated from PDA and were tested for expression of MR1 specific tetramer (5-OP-RU), compared to control tetramer (6-FP). Representative contour plots are shown. **(g, h)** Orthotopic KPC tumors were harvested from WT mice on day 21. $CD45^+CD3^+$ leukocytes were purified by FACS and analyzed by single cell RNAseq. Violin plots comparing normalized log expression of (g) *Ccr7* and (h) *Il2rb* in each lymphocyte cluster are shown. **(i, j)** Orthotopic KPC tumors were harvested from WT mice. Select lymphocyte subsets were analyzed by flow cytometry for expression of (i) CCR7 and (j) IL-2rb. This experiment was performed in 10 replicates per group. **(k)** Heat map depicting top 50 transcriptomic changes in the iαβT and NKT clusters (*$p<0.05$, **$p<0.01$, ****$p<0.0001$).

Figure S2

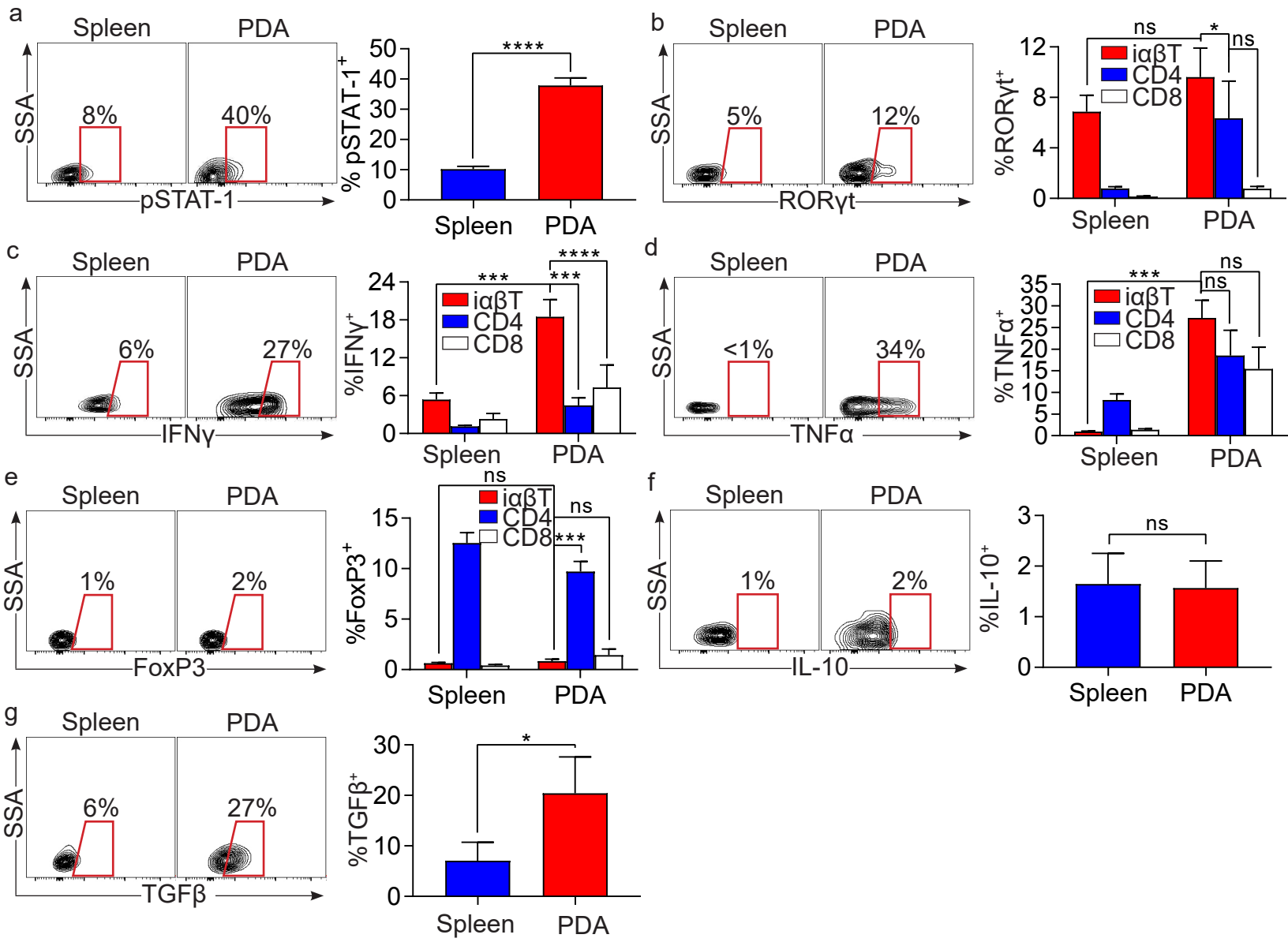
a
Spleen
PDA
SSA
8%
40%
pSTAT-1
% pSTAT-1+
****
Spleen
PDA
b
Spleen
PDA
SSA
5%
12%
RORγt
%RORγt+
ns
*
ns
iαβT
CD4
CD8
Spleen
PDA
c
Spleen
PDA
SSA
6%
27%
IFNγ
%IFNγ+
***
***
****
iαβT
CD4
CD8
Spleen
PDA
d
Spleen
PDA
SSA
<1%
34%
TNFα
%TNFα+
***
ns
ns
iαβT
CD4
CD8
Spleen
PDA
e
Spleen
PDA
SSA
1%
2%
FoxP3
%FoxP3+
ns
iαβT
CD4
CD8
***
ns
Spleen
PDA
f
Spleen
PDA
SSA
1%
2%
IL-10
%IL-10+
ns
Spleen
PDA
g
Spleen
PDA
SSA
6%
27%
TGFβ
%TGFβ+
*
Spleen
PDA

Figure S2. iαβTs exhibit a distinct phenotype in PDA and are the dominant IL-17 producing T cells. (a) Splenic and orthotopic PDA-infiltrating iαβTs were tested for expression of pSTAT-1. **(b-e)** Splenic and PDA-infiltrating iαβTs , $CD4^+$ T cells, $CD8^+$ T cells were tested for expression of (b) RORγt, (c) IFNγ, (d) TNFα, and (e) FoxP3. **(f, g)** Splenic and orthotopic PDA-infiltrating iαβTs were tested for expression of (f) IL-10 and (g) TGFβ. Each experiment was repeated at least 4 times (n=5/group; *p<0.05, **p<0.01, ***p<0.001, ****p<0.0001).

Figure S3

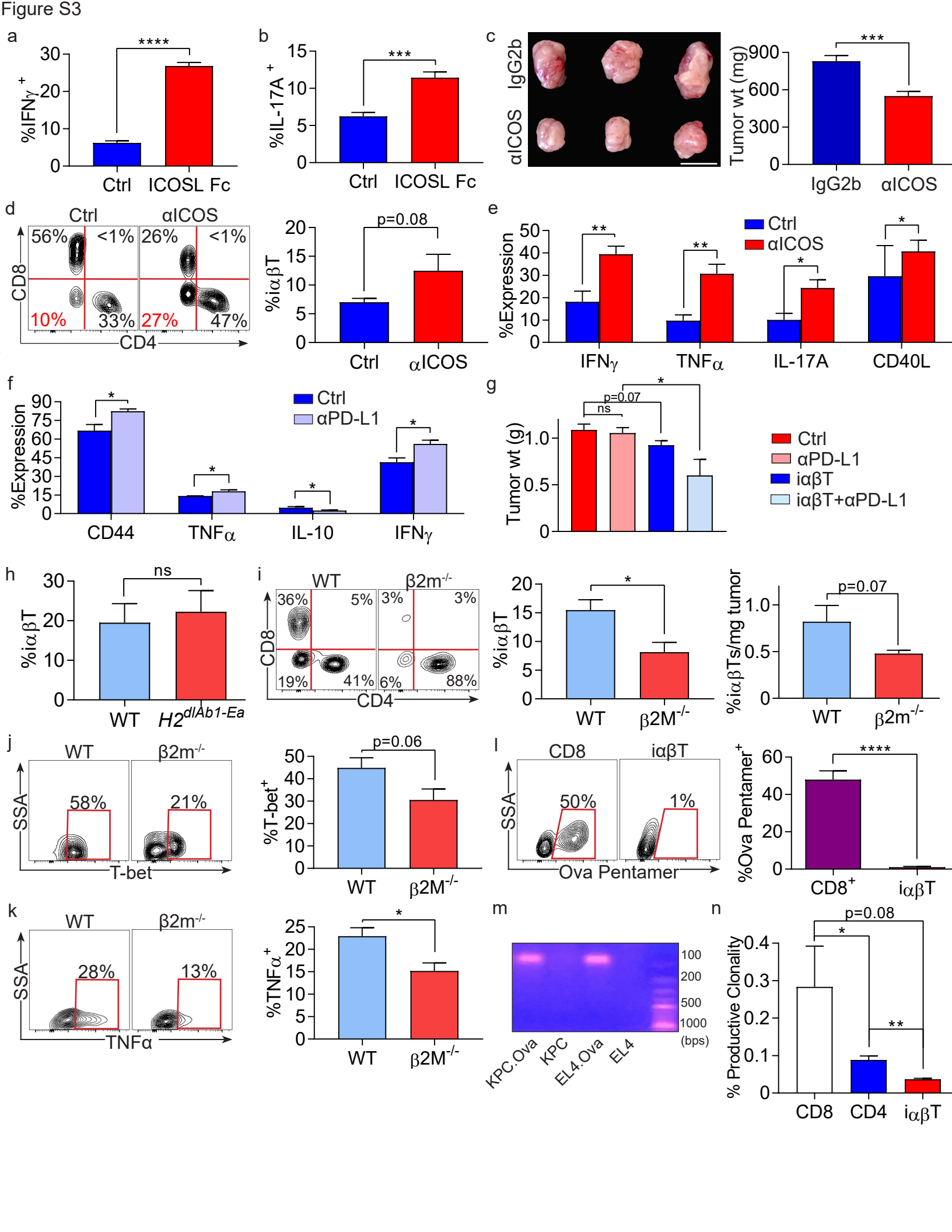
a
%IFNγ+
****
Ctrl
ICOSL Fc
b
%IL-17A+
***
Ctrl
ICOSL Fc
c
IgG2b
αICOS
Tumor wt (mg)
***
IgG2b
αICOS
d
Ctrl
αICOS
56%
<1%
26%
<1%
10%
33%
27%
47%
CD8
CD4
%iαβT
p=0.08
Ctrl
αICOS
e
%Expression
Ctrl
αICOS
IFNγ
TNFα
IL-17A
CD40L
f
%Expression
Ctrl
αPD-L1
CD44
TNFα
IL-10
IFNγ
g
Tumor wt (g)
p=0.07
ns
Ctrl
αPD-L1
iαβT
iαβT+αPD-L1
h
%iαβT
ns
WT
H2dlAb1-Ea
i
WT
β2m-/-
36%
5%
3%
3%
19%
41%
6%
88%
CD8
CD4
%iαβT
WT
β2M-/-
%iαβTs/mg tumor
p=0.07
WT
β2m-/-
j
WT
β2m-/-
58%
21%
SSA
T-bet
%T-bet+
p=0.06
WT
β2M-/-
l
CD8
iαβT
50%
1%
SSA
Ova Pentamer
%Ova Pentamer+
****
CD8+
iαβT
k
WT
β2m-/-
28%
13%
SSA
TNFα
%TNFα+
*
WT
β2M-/-
m
100
200
500
1000
(bps)
KPC.Ova
KPC
EL4.Ova
EL4
n
% Productive Clonality
p=0.08
*
**
CD8
CD4
iαβT

Figure S3. iαβTs are activated by checkpoint and costimulatory receptor targeted immunotherapies. (a, b) Splenic iαβTs were activated *in vitro* with plate-bound αCD3 in the presence of ICOSL Fc or vehicle for 72h and tested for expression of (a) IFNγ and (b) IL-17A. This experiment was repeated twice in replicates of 5. **(c-e)** Orthotopic PDA-bearing WT mice were serially treated with an agonizing αICOS mAb or isotype control. Tumors were harvested at 21days (n=5/group). (c) Representative pictures of tumors and quantitative analysis of tumor weights are shown. (d) The fraction of $CD4^+$, $CD8^+$, and iαβTs among $TCR\beta^+NK1.1^-$ T cells was determined in the ICOS agonist treated and control groups. Representative contour plots and quantitative data are shown. (e) iαβT cell expression of IFNγ, TNFα, IL-17A, and CD40L were measured in each cohort. **(f)** Orthotopic PDA-bearing WT mice were serially treated with an neutralizing αPD-L1 mAb or isotype control (n=5/group). Tumors were harvested at 21 days and tumor-infiltrating iαβT cell expression of CD44, TNFα, IL-10, and IFNγ were measured in each cohort. Each *in vivo* experiment was repeated more than 3 times. **(g)** Orthotopic PDA-bearing WT mice were serially treated with an neutralizing αPD-L1 mAb alone, iαβT cell transfer alone, or both in combination. Tumor weight on day 21 is shown (n=5/group). **(h)** Orthotopic PDA-bearing WT and $MHCII^{-/-}$ mice were analyzed for the frequency of tumor-infiltrating iαβT cells among all $TCR\beta^+$ T cells. **(i-k)** Orthotopic PDA-bearing WT and $\beta2m^{-/-}$ mice were analyzed for (i) the frequency of tumor-infiltrating iαβTs, and (j) iαβT cell expression of T-bet and (k) TNFα. Representative contour plots and quantitative data are shown (n=5/group). This experiment was repeated 3 times. **(l, m)** WT mice were orthotopically implanted with KPC-derived tumor cells engineered to express Ovalbumin (KPC.Ova). (l) On day 21, KPC.Ova tumors were harvested, digested, and $CD8^+$ T cells and iαβTs were assayed using an $Ova_{257-264}$-Pentamer. Representative contour plots and quantitative data are shown (n=5/group). (m) PCR for Ovalbumin expression in KPC and KPC.Ova tumors are shown. EL4 and EL4.Ova tumor cells were used as controls. **(n)** TCR Sequencing was performed in triplicate on PDA-infiltrating $CD4^+$, $CD8^+$, and iαβTs and populations were assessed for productive clonality (*$p<0.05$, **$p<0.01$, ***$p<0.001$, ****$p<0.0001$).

Figure S4

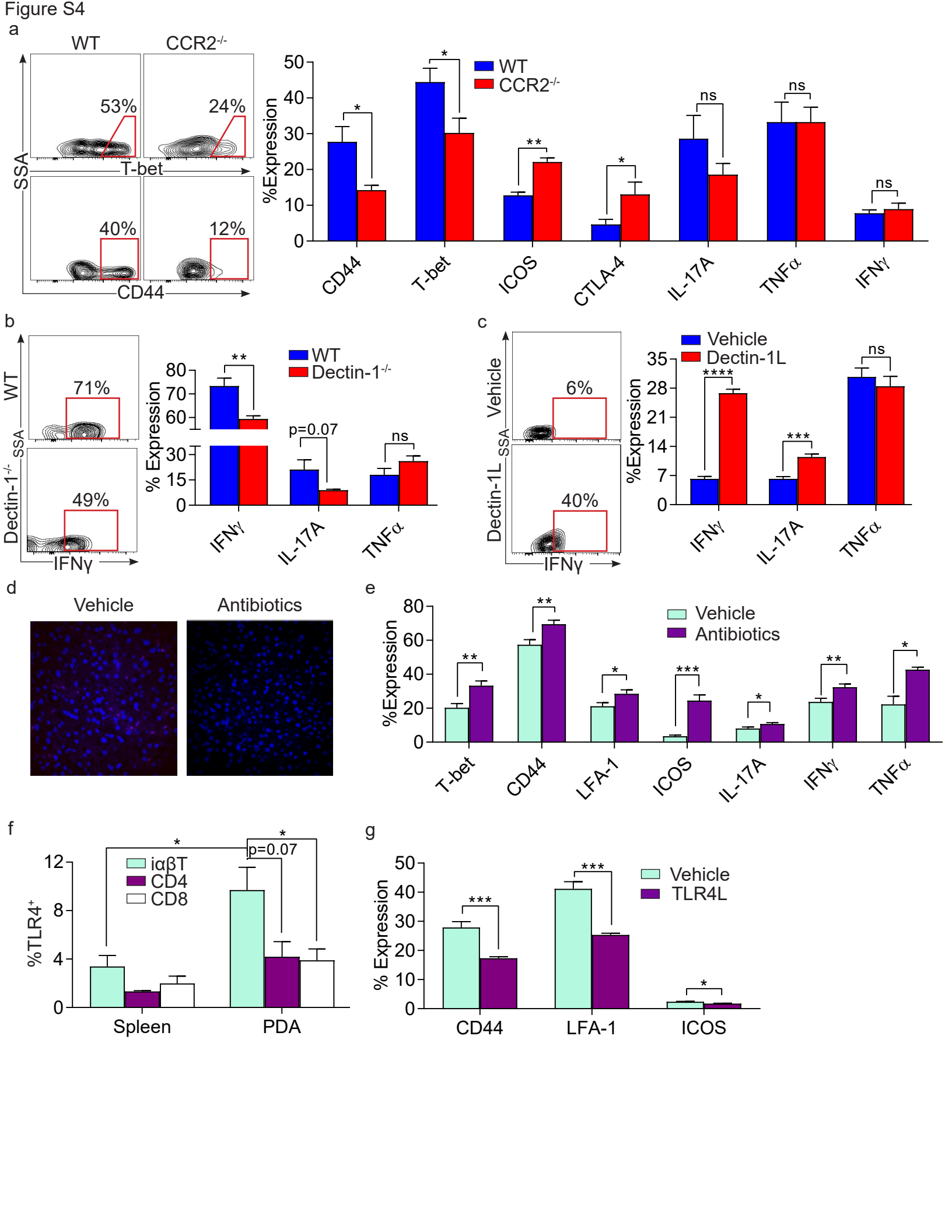
a
WT
CCR2-/-
53%
24%
40%
12%
SSA
T-bet
CD44
%Expression
WT
CCR2-/-
CD44
T-bet
ICOS
CTLA-4
IL-17A
TNFα
IFNγ
b
WT
71%
Dectin-1-/-
49%
SSA
IFNγ
% Expression
WT
Dectin-1-/-
p=0.07
ns
IFNγ
IL-17A
TNFα
c
Vehicle
6%
Dectin-1L
40%
SSA
IFNγ
%Expression
Vehicle
Dectin-1L
ns
IFNγ
IL-17A
TNFα
d
Vehicle
Antibiotics
e
%Expression
Vehicle
Antibiotics
T-bet
CD44
LFA-1
ICOS
IL-17A
IFNγ
TNFα
f
%TLR4+
iαβT
CD4
CD8
p=0.07
Spleen
PDA
g
% Expression
Vehicle
TLR4L
CD44
LFA-1
ICOS

Figure S4. Selective modulation of iαβT cell phenotype by sterile and microbial signals. (a) Orthotopic PDA tumors were harvested from WT and CCR2$^{-/-}$ mice. iαβTs were gated on flow cytometry and tested for expression of CD44, T-bet, ICOS, CTLA-4, IL-17A, TNFα, and IFNγ (n=5/group). This experiment was repeated 3 times. **(b)** Orthotopic PDA tumors were harvested from WT and Dectin-1$^{-/-}$ mice on day 21 and tested for expression of IFNγ, IL-17, and TNFα. Select representative contour plots and quantitative data are shown. This experiments was performed in replicates of 5 and repeated 3 times. **(c)** Splenic iαβTs from naïve WT were harvested and activated *in vitro* by CD3 ligation, either alone or in the presence of the Dectin-1 ligand depleted zymosan. iαβT cell expression of IFNγ, IL-17A, and TNFα was determined at 72h. Select representative contour plots and quantitative data are shown. This experiment was performed in replicates of 5 and repeated 3 times. **(d)** Bacterial abundance in PDA tumors in control and oral antibiotic-treated mice was tested by 16S rRNA FISH. **(e)** PDA-infiltrating iαβTs in control and oral antibiotic-treated hosts were tested for expression of (e) T-bet, CD44, LFA-1, ICOS, IL-17A, IFNγ, and TNFα. Representative contour plots and quantitative data are shown. This experiment was repeated 3 times (n=5/group). **(f)** Splenic and orthotopic PDA-infiltrating iαβTs, CD4$^+$ T cells, and CD8$^+$ T cells, and were tested for expression of TLR4 (n=5 mice). **(g)** Orthotopic PDA-bearing WT mice were serially treated i.p. with TLR4 ligand LPS or vehicle and iαβTs were harvested and tested for expression of CD44, LFA-1, and ICOS (n=5/group). This experiment was repeated 3 times (*p<0.05, **p<0.01, ***p<0.001, ****p<0.0001).

Figure S5

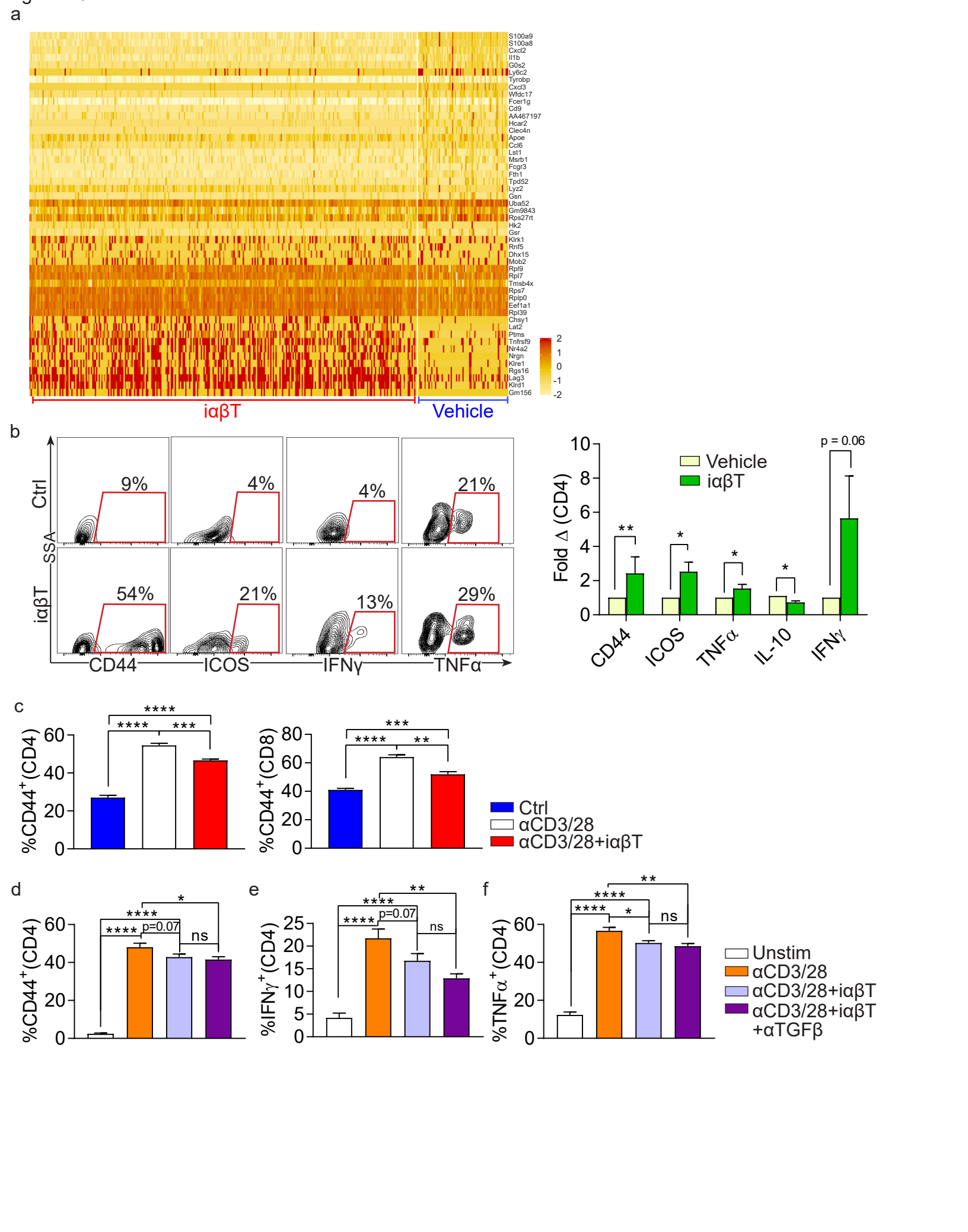
a
S100a9
S100a8
Cxcl2
Il1b
G0s2
Ly6c2
Tyrobp
Cxcl3
Wfdc17
Fcer1g
Cd9
AA467197
Hcar2
Clec4n
Apoe
Ccl6
Lst1
Msrb1
Fcgr3
Fth1
Tpd52
Lyz2
Gsn
Uba52
Gm9843
Rps27rt
Hk2
Gsr
Klrk1
Rnf5
Dhx15
Mob2
Rpl9
Rpl7
Trmsb4x
Rps7
Rplp0
Eef1a1
Rpl39
Chsy1
Lat2
Ptms
Tnfrsf9
Nr4a2
Nrgn
Klre1
Rgs16
Lag3
Klrd1
Gm156
2
1
0
-1
-2
iαβT
Vehicle
b
Ctrl
iαβT
SSA
9%
4%
4%
21%
54%
21%
13%
29%
CD44
ICOS
IFNγ
TNFα
Fold Δ (CD4)
Vehicle
iαβT
p = 0.06
CD44
ICOS
TNFα
IL-10
IFNγ
c
%CD44+(CD4)
%CD44+(CD8)
Ctrl
αCD3/28
αCD3/28+iαβT
d
%CD44+(CD4)
p=0.07
ns
e
%IFNγ+(CD4)
p=0.07
ns
f
%TNFα+(CD4)
ns
Unstim
αCD3/28
αCD3/28+iαβT
αCD3/28+iαβT
+αTGFβ

Figure S5. iαβTs enhance adaptive immunity in murine and human PDA but regulate conventional T cell activation *in vitro*. (a) Mice with established orthotopic KPC tumor were serially transferred i.v. twice weekly with iαβTs or vehicle beginning on day 5. Mice were sacrificed at day 21 and single cell RNAseq was performed on FACS-purified $CD45^+$ tumor-infiltrating leukocytes. The distribution of cellular clusters was determined using the t-SNE algorithm. A heat map indicates the top 50 differentially expressed genes in the T cell cluster between the two treatment groups. **(b)** PDOTS derived from resected human tumors were treated with autologous iαβTs or vehicle. $CD4^+$ T cells were analyzed for expression of CD44, ICOS, IFNγ, TNFα, and IL-10. Representative contour plots from human PDA PDOTS experiment and quantitative data indicating fold-change in expression the $CD4^+$ T cells in iαβT-treated PDOTS compared to vehicle-treated PDOTS are shown (n=5 patients). **(c)** Polyclonal $CD4^+$ and $CD8^+$ T cells were cultured without stimulation, stimulated by CD3/CD28 co-ligation, or stimulated by CD3/CD28 co-ligation in co-culture with iαβTs. $CD4^+$ and $CD8^+$ T cell activation were determined at 72h by expression of CD44. This experiment was repeated 4 times in replicates of 5. (**d-f**) Polyclonal $CD4^+$ T cells were cultured without stimulation or stimulated by CD3/CD28 co-ligation, alone or in co-culture with iαβTs. A neutralizing α-TGFβ mAb or isotype control was added to select wells. $CD4^+$ T cell activation was determined at 72h by expression of (d) CD44, (e) IFNγ and (f) TNFα. This experiment was repeated twice in replicates of 5 (*$p<0.05$, **$p<0.01$, ***$p<0.001$, ****$p<0.0001$).

Figure S6

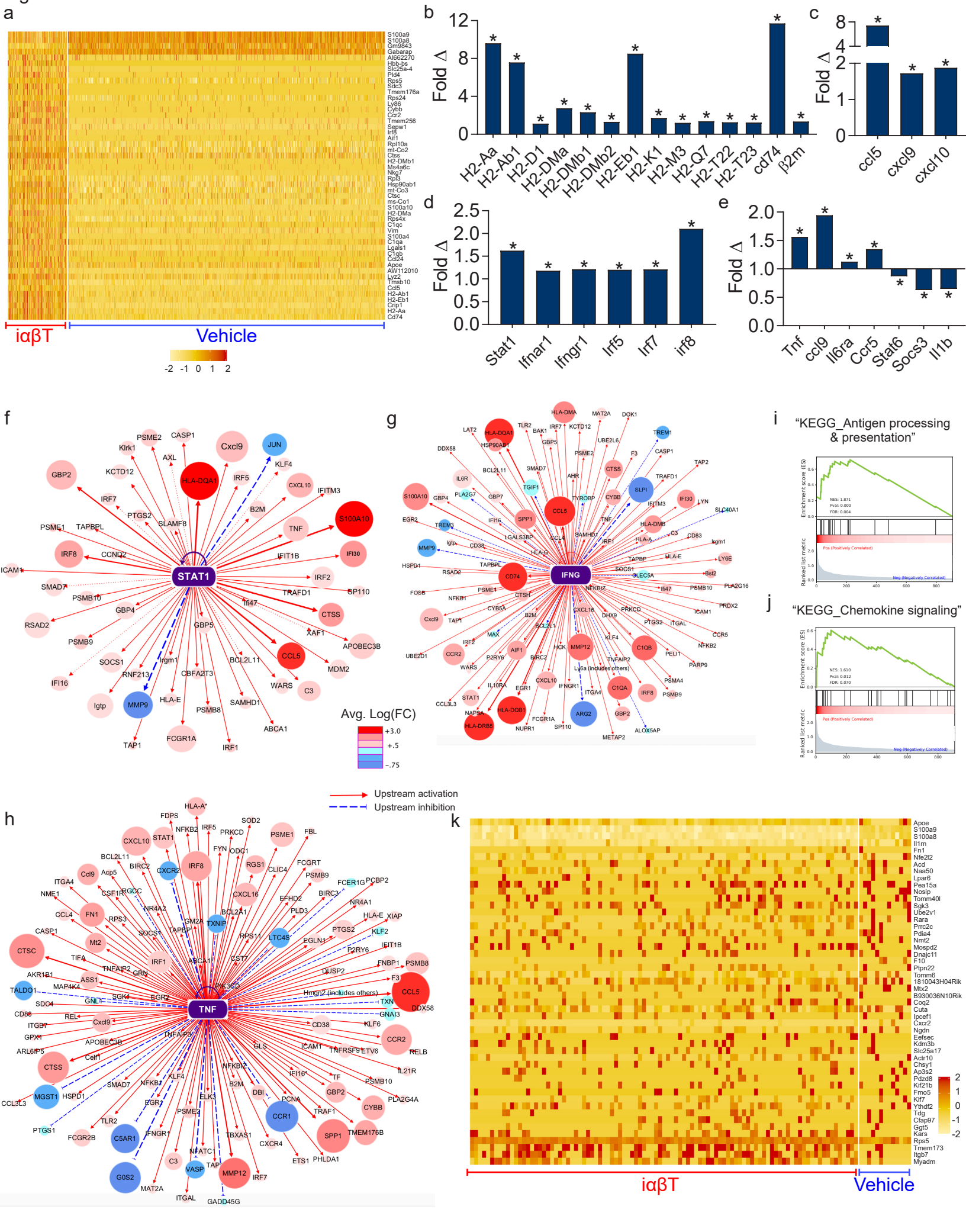
a
iαβT
Vehicle
-2 -1 0 1 2
b
Fold Δ
H2-Aa
H2-Ab1
H2-D1
H2-DMa
H2-DMb1
H2-DMb2
H2-Eb1
H2-K1
H2-M3
H2-Q7
H2-T22
H2-T23
cd74
β2m
c
Fold Δ
ccl5
cxcl9
cxcl10
d
Fold Δ
Stat1
Ifnar1
Ifngr1
Irf5
Irf7
irf8
e
Fold Δ
Tnf
ccl9
Il6ra
Ccr5
Stat6
Socs3
Il1b
f
STAT1
Avg. Log(FC)
+3.0
+.5
-.75
g
IFNG
i
"KEGG_Antigen processing & presentation"
Enrichment score (ES)
NES: 1.871
Pval: 0.000
FDR: 0.004
Pos (Positively Correlated)
Neg (Negatively Correlated)
Ranked list metric
j
"KEGG_Chemokine signaling"
NES: 1.610
Pval: 0.012
FDR: 0.070
h
Upstream activation
Upstream inhibition
TNF
k
iαβT
Vehicle

Figure S6. iαβT adoptive transfer confers an immunogenic phenotype in TAMs. (a) Mice with established orthotopic KPC tumor were serially transferred i.v. twice weekly with iαβTs or vehicle beginning on day 5. Mice were sacrificed at day 21 and single cell RNAseq performed on FACS-purified $CD45^+$ tumor-infiltrating leukocytes. The distribution of cellular clusters was determined using the t-SNE algorithm. A heat map indicates the top 50 differentially expressed genes in the macrophage cluster between the two treatment groups. **(b-e)** Differential expression (iαβT vs vehicle) of select genes in the macrophage cluster related to (b) antigen-presentation, (c) T cell chemoattraction, (d) IFN signaling, and (e) macrophage polarization. **(f-h)** Bubble plots depicting upstream activation of (f) STAT1, (g) TNFα, and (h) IFNγ signaling based on ingenuity pathway analysis of upstream regulators in macrophages infiltrating iαβT cell-treated PDA tumors compared with vehicle treatment. **(i, j)** GSEA showing enrichment of (i) "KEGG_Antigen processing and presentation" and (j) "KEGG_Chemokine signaling pathway" in the macrophage cluster in iαβT cell-treated PDA. **(k)** A heat map indicates the top 50 differentially expressed genes in the $CX3CR1^+$ Macrophage cluster between the two treatment groups (*$p<0.0001$).

Figure S7

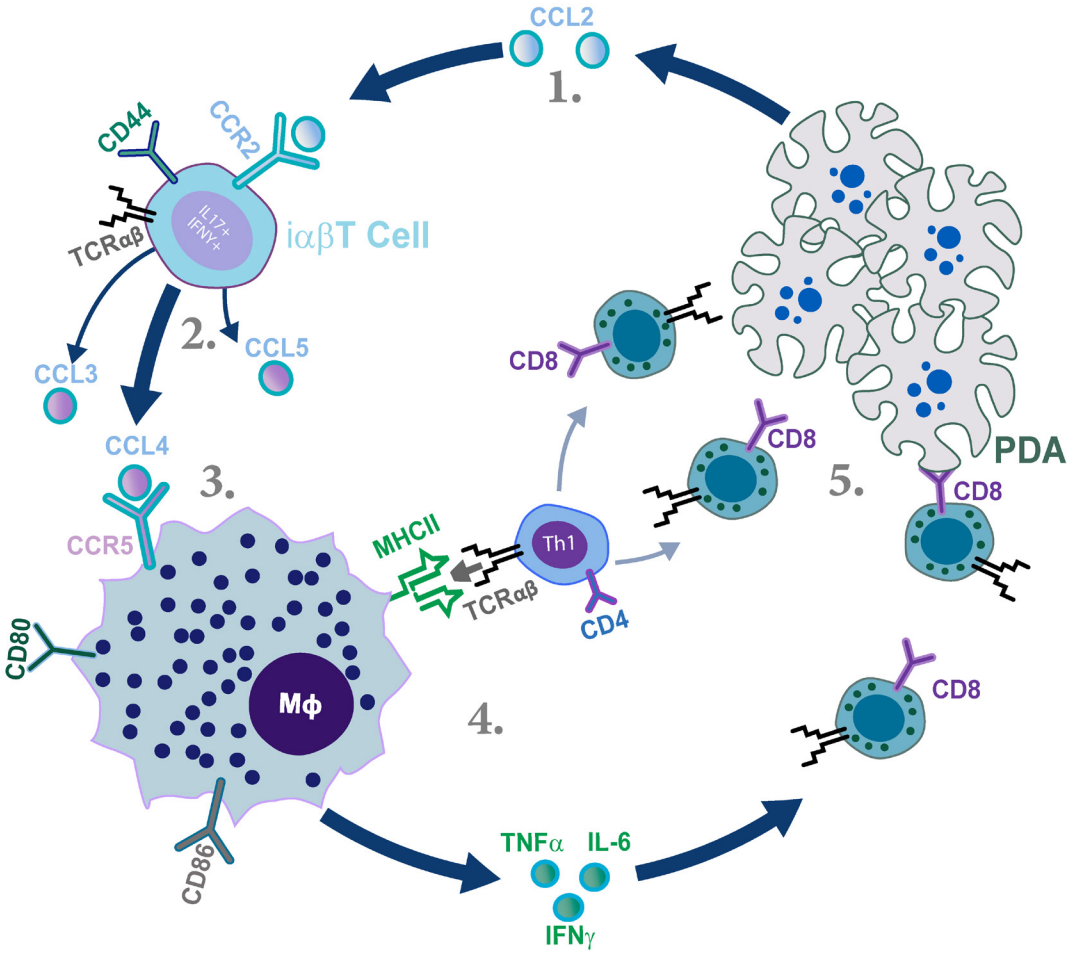
CCL2
1.
CD44
CCR2
IL17+
IFNγ+
TCRαβ
iαβT Cell
2.
CCL3
CCL5
CD8
PDA
CD8
CD8
5.
CCL4
3.
CCR5
MHCII
Th1
TCRαβ
CD4
CD80
Mφ
4.
CD8
CD86
TNFα
IL-6
IFNγ

Figure S7. Schematic depicting recruitment and immunogenic properties of iαβTs in PDA. 1. Tumor derived CCL2 recruits iαβT cells to the PDA TME. 2. PDA-infiltrating iαβT cells secrete CCR5 ligands. 3. CCL3, CCL4, and CCL5 bind to CCR5 on TAMs and induce an M1-phenotype. 4. Activated TAMs promote immunogenic $CD4^+$ and $CD8^+$ differentiation and expansion. 5. Cytotoxic $CD8^+$ T cells induce tumor cell death.